Experimental Study of the Sb-Sn-Zn Alloy System

Ondrej Zobac, Jiri Sopousek, Jiri Bursik, Adela Zemanova & Pavla Roupcova

Metallurgical and Materials Transactions A

ISSN 1073-5623

Metall and Mat Trans A
DOI 10.1007/s11661-013-2104-1

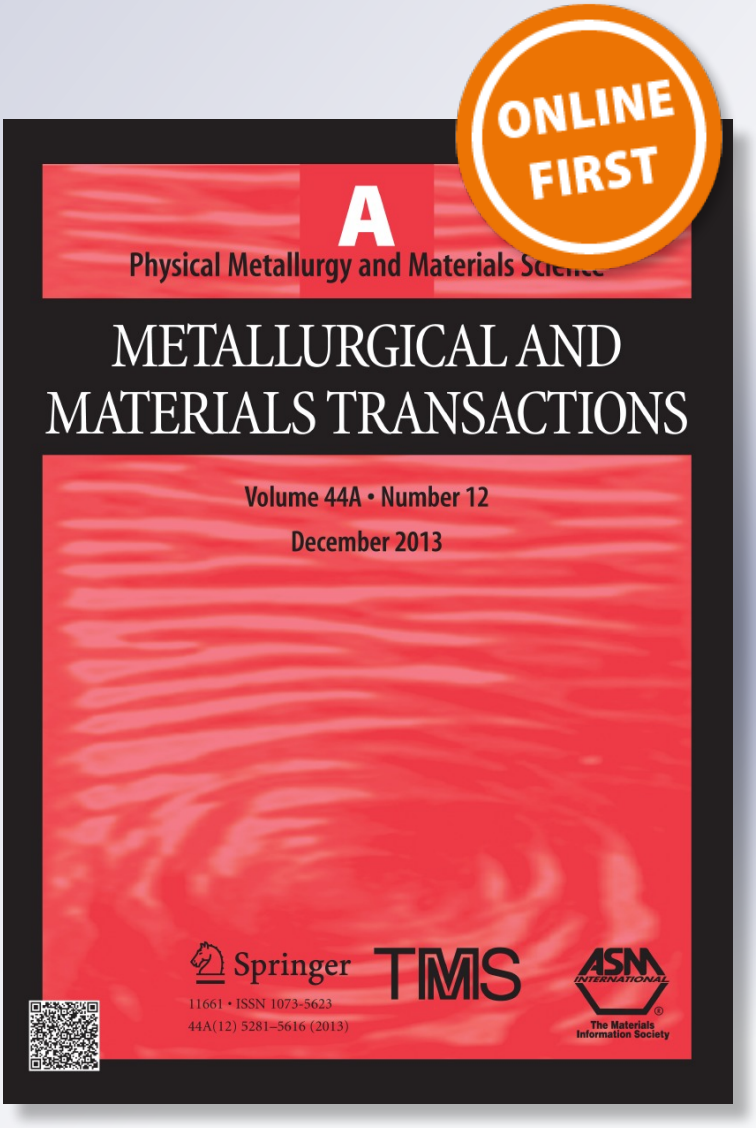

Springer

Experimental Study of the Sb-Sn-Zn Alloy System

ONDREJ ZOBAC, JIRI SOPOUSEK, JIRI BURSIK, ADELA ZEMANOVA, and PAVLA ROUPCOVA

The Sb-Sn-Zn alloy was prepared and researched by experimental methods, which allow obtaining information on the thermodynamic stability of the coexisting phases. Thermal analysis was used to determine the phase transition temperatures of experimental alloys. Equilibrium composition of coexisting phases after long-term temperature equilibration was determined by electron microscopy. The existence of one ternary stoichiometric phase Sb_2SnZn was experimentally confirmed by diffraction technique. The CALPHAD method for prediction of the phase diagram of the Sb-Sn-Zn system from binary subsystems was used in this work.

DOI: 10.1007/s11661-013-2104-1

I. INTRODUCTION

TIN, antimony, and zinc are easily fusible metals used in many technical industries and areas of technology. Tin is mainly used as the major component of low-melting solders.[1] Antimony and zinc are metals which can also be found in the solder alloy.[2] The commonly used Sn-Pb solder has been replaced by lead-free solders for environmental and health reasons. The most widely used lead-free solders for low-temperature soldering are Sn-Ag-Cu-based alloys (SAC solders).[3,4] Aside from the already established low-temperature lead-free solders there is still undergoing materials research of new alloys for brazing. Antimony and zinc are a common part of developed alloys for lead-free soldering.[5,6]

An important source of information for the proposal of new alloys is the equilibrium phase diagram.[7] Details about coexistence and stability of phases including liquidus phase significantly streamline this material research. For this reason, this work pays special attention to experimental description of the Sb-Sn-Zn ternary system. Binary diagrams of Sb-Sn, Sn-Zn, and Sb-Zn[7] subsystems are known and they are described in great detail in Reference 8, 9. However, only little experimental information concerning Sb-Sn-Zn ternary alloy is known and experimental description of this system needs to be expanded. Some works dealing with thermodynamic phase coexistence in the ternary system were published in the period 1976 to 2011. The works dealt with the phase diagram of the Sb-Sn-Zn system,[10] structure of Sb_2SnZn intermetallic phase[11] and metal activities in ternary liquid.[12] Some older sources[10,13,14] reported studies of the Sb-Sn-Zn system on account of the use of the ternary intermetallic phase Sb_2SnZn as a semiconductor.

An important milestone of material research of alloys was the CALPHAD method developed in 1975[15] which was further developed (extended-generalized-adopted) for alloys.[16] The method is based on a thermodynamic description of the phases, which are described and parametrically stored in specialized databases.[7]

Phase diagrams are possible to calculate using several different CALPHAD-based programs *e.g.*, Thermo-Calc[17] or Pandat.[18] Relevant thermodynamic database can be used to calculate equilibrium phase diagrams of binary subsystems, here Sb-Sn,[9] Sn-Zn,[7] and Sb-Zn.[8] The method also allows us to predict the ternary phase diagram of the Sb-Sn-Zn system, as the authors used before[19] and here for better understanding of the obtained experimental results.

The CALPHAD method provides a prediction of stable phase diagram of the ternary system from binary subsystems. It fails, however, when the ternary system contains a ternary phase. This problem can also be observed in the Sb-Sn-Zn system where the stoichiometric ternary phase Sb_2SnZn was experimentally observed.[10] Specification of the stability range of the ternary phase and positioning of the phase fields with mutual solubility of all three components was the motivation for the experimental study of Sb-Sn-Zn ternary system. Chemical and phase analysis of coexisting phases in Sb-Sn-Zn alloys were performed. Moreover, differential thermal analysis (DTA) was used for phase transformation study.

II. EXPERIMENTAL PROCEDURE

The overall composition of the samples was chosen with regard to the predicted isothermal sections of Sb-Sn-Zn phase diagram. Figures 1, 2, and 3 show isothermal sections of Sb-Sn-Zn phase diagram for temperatures 473 K, 523 K, and 623 K (200 °C, 250 °C, and 350 °C) with marked overall composition of samples as black points. The CALPHAD approach

ONDREJ ZOBAC, Ph.D. Student, and JIRI SOPOUSEK, Associate Professor, are with the CEITEC, Masaryk University, Brno, Czech Republic, and also with the Department of Chemistry, Faculty of Sciences, Masaryk University. Contact e-mail: ondrej.zobac@gmail.com JIRI BURSIK, ADELA ZEMANOVA, and PAVLA ROUPCOVA, Researchers, are with the Institute of Physics of Materials, ASCR, Brno, Czech Republic.

Manuscript submitted January 20, 2013.

Published online: 08 November 2013

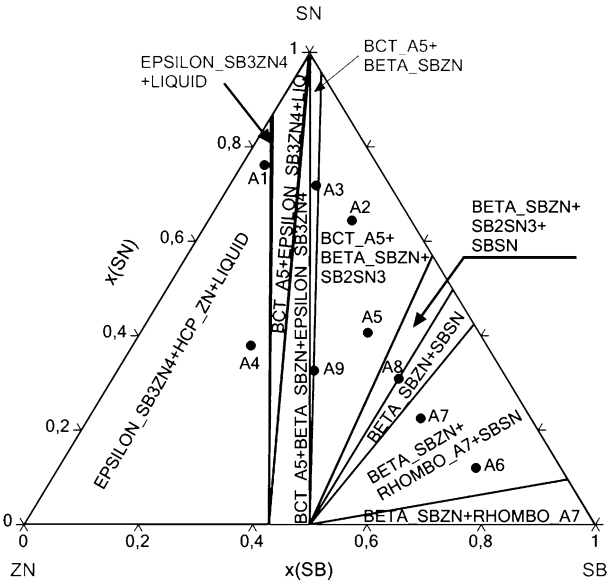

Fig. 1—Isothermal cross sections of the phase diagram of the Sn-Sb-Zn system at 473 K (200 °C) calculated from Sb-Sn, Sb-Zn, and Sn-Zn binaries. Overall compositions of the experimental alloys (black points) are plotted.

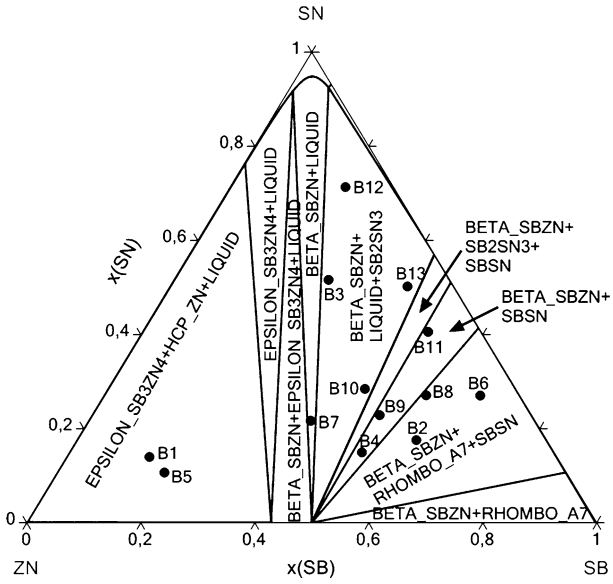

Fig. 2—Isothermal cross sections of the phase diagram of the Sn-Sb-Zn system at 523 K (250 °C) calculated from binaries. Overall compositions of the experimental alloys (black points) are plotted.

implemented in the PANDAT 2012 program was used for the prediction of isothermal sections of Sb-Sn-Zn phase diagrams. COST 531 database optimized for solders (SOLDER) and updated with the published information about Sb-Sn[9] and Sb-Zn[8] subsystems was used for the calculation of phase diagrams.

The samples of alloys were prepared from pure metals (with purity higher than 99.999 pct). The weighed pure metals were transferred into quartz ampoules and sealed under vacuum (~0.1 mBar). Two kinds of quartz ampoules were used. The first type was the common quartz ampoule suitable for long-term annealing of alloys with a total weight of 2 to 5 g. The second type (DTA Ampoules) was prepared (total weight of the sample about 0.75 g) in order to be suitable for both measuring the DTA signal of the experimental alloys and to follow long-term annealing. The samples of alloys for all consequent studies were taken from the center of the material due to the possibility of surface oxidation of metals, especially zinc.

The samples inside common and DTA ampoules were heat-treated in slightly different ways. The pure metals inside the common quartz ampoules were melted at 923 K (650 °C) and homogenized by manual shaking. Melting and shaking was repeated several times until the alloys became homogeneous. Ampoules with homogeneous alloys were loosely cooled to the room temperature. The two sets of samples were prepared in evacuated common quartz ampoules for long-term annealing. The molar ratios of Sb, Sn, and Zn were selected to evenly cover the phase field in isothermal

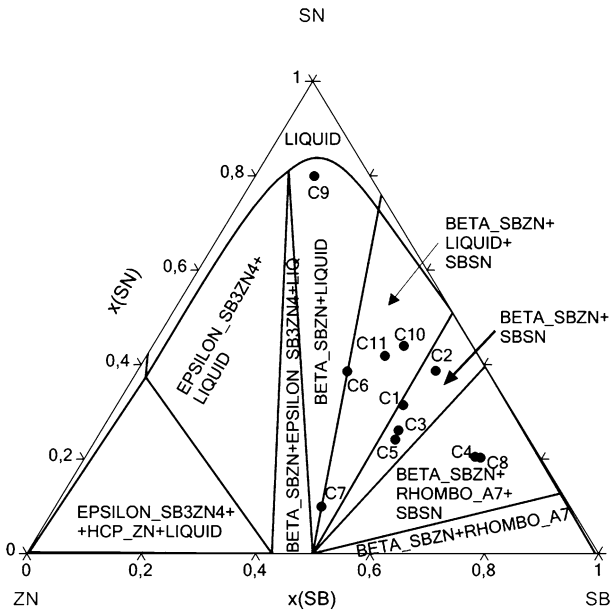

Fig. 3—Isothermal cross sections of the phase diagram of the Sn-Sb-Zn system at 623 K (350 °C) calculated from binaries. Overall compositions of the experimental alloys (black points) are plotted.

sections of the approximate phase diagram at 473.15 K and 523.15 K (200 °C and 250 °C). The first set of samples was placed into a LAC 1200 furnace and annealed at 473 K ± 1 K (200 °C ± 1 °C)/500 h. The second set of samples was placed in the same furnace and annealed at 523 K ± 1 K (250 °C ± 1 °C)/1700 h.

Table I. Temperatures of Phase Transitions Obtained by DTA

Sample	Overall Composition (at. pct)			Liquidus Temperature [K (°C)]	Other Phase Transition Markers [K(°C)]					
	x(Sb)	*x*(Sn)	*x*(Zn)							
C1	50.10	31.45	18.45	**713.2 (440.0)**	504.8 (231.6)	586.9 (313.7)	643.6 (370.4)	654.5 (381.3)	666.7 (393.5)	
C2	52.15	38.71	9.14	**661.7 (388.5)**	509.9 (236.7)	586.5 (313.3)	641.2 (368.0)			
C3	51.95	26.10	21.95	**775.3 (502.1)**	510.4 (237.2)	590.4 (317.2)	632.5 (359.3)	647.3 (374.1)	**670.9 (397.7)**	737 (463.8)
C4	68.17	20.48	11.35	**782.2 (509.0)**	666.9 (393.7)	698.2 (425.0)	719.1 (445.9)			
C5	52.38	24.13	23.49	**751.0 (477.8)**	510.3 (237.1)	595.7 (322.5)	646.1 (372.9)	657 (383.8)	**678.9 (405.7)**	706.2 (433.0)
C6	36.75	38.59	24.66	**798.6 (525.4)**	469.2 (196.0)	501.3 (228.1)				
C7	46.55	9.95	43.50	**768.7 (495.5)**	650.7 (377.5)	662.9 (389.7)	709.4 (436.2)			
C8	69.20	20.31	10.96	**739.2 (466.0)**	470.4 (197.2)	494.0 (220.8)	515.4 (242.2)	621.7 (348.5)	716.5 (443.3)	
C9	10.31	79.93	9.76	**514.3 (241.1)**	469.1 (195.9)	474.6 (201.4)				
C10	43.95	44.00	12.05	**598.9 (325.7)**	496.8 (223.6)	511.3 (238.1)	516.0 (242.8)	590.2 (317.0)		
C11	41.69	41.88	16.43	**619.5 (346.3)**	468.4 (195.2)	511.4 (238.2)	590.2 (317.0)	596.7 (323.5)	596.4 (323.2)	

Intense endothermic minima are given in bold.

The cooling of the samples after annealing was carried out by dropping them rapidly into cold water which caused the ampoule to break instantly.

The samples inside DTA ampoules were prepared to fit the space in STA 409CD/3/403/5/G calorimeter (Netzsch). Homogeneous alloys in the DTA quartz ampoules were analyzed by the DTA method at the rate of 5 K/min and cooled down at the same rate. This heat treatment cycle was repeated three times for each ampoule-encapsulated sample. The measurement was carried out under standard conditions inside a calorimeter (6 N argon, flow 70 mL/min).[20] The DTA signal was evaluated by "Proteus Thermal Analysis" software provided by NETZSCH Company. An example of the evaluation of the DTA curve of the alloy is shown in Figure 1. Average temperatures of phase transitions of the heating curves of the second and third cycles were evaluated and noted in Table I that summarizes temperatures of the phase transitions.

The samples which were measured by DTA were exploited once more. The DTA ampoules with an alloy sample inside were equilibrated in a furnace at 623 K ± 1 K (350 °C ± 1 °C)/(450 to 1000 h) to reach a state near thermodynamic equilibrium. A different way was used for the sample C5, which was annealed after DTA measurement in calorimeter STA 409 at 623 K ± 1 K (350 °C ± 1 °C) for 9 hours. The cooling of all the samples after prolonged annealing was carried out by ampoule breaking in water.

All quenched samples equilibrated at 473 K, 523 K, and 623 K (200 °C, 250 °C, and 350 °C) were cut in the center and metallographically polished and investigated by methods of electron microscopy. A JEOL 6460 scanning electron microscope (SEM) with INCA Energy analyzer was used. The overall composition of the samples and the composition of the coexisting phases were measured by energy-dispersive X-ray analysis (EDX microanalysis). The results are shown in Table II 473 K (200 °C), Table III 523 K (250 °C), and Table IV 573 K (350 °C). The names of the individual phases were taken from literature.[7] The phase names are: Rhombo_A7, BCT_A5, HCP_Zn, SbSn, SbZn_Beta, Sb_2SnZn, and liquid (an alternative labeling in the same sequence: βSb, βSn, Zn, β, β, -, -; Pearson symbols hR2, tI4, hP2, cF8, oP16, -, -).

The polished areas of the equilibrated samples were investigated by means of EDX in SEM. The microanalysis was elementary because the equilibrated phases formed big grains and were a different shade of gray. The two- and three-phase coexistences were mostly found (see Table IV). For example, the samples C2 and C10 reveal three-phase microstructure as shown in Figures 4 and 5.

Phase identification at room temperature using Rigaku XRD analyser was applied to representative samples. The presence of binary phases including Sb_2SnZn ternary compound was confirmed. The equilibrating liquid phase turns to solid after quenching and identified as βSn eventually as βSb solid solution. An example of X-ray diffraction spectrum for sample B10 is shown in Figure 6.

Table II. The Overall Composition and Composition of Coexisting Phases at 473 K (200 °C)[21]

	Overall Composition (at. pct)				Phases Composition (at. pct)		
Sample	Sb	Sn	Zn	Coexisting Phases	Sb	Sn	Zn
A1	4.02	76.14	19.84	HCP_Zn	0.00	0.37	99.63
				HCP_Zn	0.31	3.44	96.25
				BCT_A5	4.94	88.49	6.58
A2	25.20	64.39	10.42	SbZn_Beta	50.29	0.00	49.71
				Sb_2SnZn	50.76	23.98	25.26
				BCT_A5	9.99	87.44	2.57
A3	15.21	71.82	12.96	SbZn_Beta	50.78	0.00	49.22
				BCT_A5	4.91	90.62	4.47
A4	20.75	37.91	41.34	HCP_Zn	0.07	0.67	99.26
				SbZn_Epsilon	40.44	0.30	59.26
				BCT_A5	4.31	91.20	4.49
A5	39.85	40.63	19.53	BCT_A5	8.88	89.27	1.86
				SbZn_Beta	52.76	0.77	46.47
				Sb_2SnZn	52.06	24.13	23.81
A6	73.07	11.99	14.94	SbZn_Beta	53.51	0.78	45.71
				SbSn	60.98	38.78	0.24
				Rhombohedral_A7	93.98	5.80	0.22
A7	58.18	22.48	19.34	SbZn_Beta	52.83	0.51	46.66
				Sb_2SnZn	52.40	23.53	24.07
				SbSn	47.54	52.31	0.15
				SbSn	63.00	36.61	0.39
A8	50.15	30.89	18.96	SbZn_Beta	52.48	0.82	46.70
				Sb_2SnZn	52.16	23.52	24.32
				SbSn	61.15	38.49	0.37
				SbSn	47.69	51.81	0.49
A9	34.48	32.61	32.92	SbZn_Beta	52.39	0.45	47.16
				BCT_A5	0.00	95.76	4.24
				BCT_A5	0.36	98.06	1.58

III. DISCUSSION

The experimental preparation of alloy samples of the Sb-Sn-Zn system requires a special technique using pre-evacuated quartz ampoules. This is due to the high vapor pressure of zinc, which can evaporate. The walls of the ampoules prevent the evaporation of Zn and thus ensure that there are no changes to the overall composition of the samples during long-term exposure. Sufficient homogenization of the melt was important as well. The advantage of samples in ampoules is also suppression of oxidation of the samples, which occurs especially when the monitored temperature is near the liquidus temperature. Samples were obtained near thermodynamic equilibrium state by using long-term annealing in quartz ampoules. The CALPHAD method has been used with advantage. This method allowed us to predict the phase diagram using the data from binary subsystems[7–9] and to plan the experiment effectively.

Experimentally, only one ternary phase was found in some samples, referred to as Sb_2SnZn. It was confirmed that within experimental error the chemical composition of the ternary phase corresponds to the expected stoichiometry (2:1:1) of the Sb_2SnZn phase.

The experimental alloys after long-term annealing showed coexistence of two or three phases in accordance with the Gibbs phase rule with the exception of sample A7 and A8 (see Table II), B8 (see Table III), C4, and C8 (see Table IV) where four phases were observed in Sb-rich region. The nonequilibrium sample B8 was investigated using XRD analysis in detail. The phase composition was: 9 wt pct Rhombo_A7 (βSb), 15 pct SbZn-beta; 33 pct Sb2SnZn, 43 pct SnSb. The increased number (4) of coexisting phases, which does not comply with Gibbs phase rule, is probably due to thermal history of Sb-rich samples before or after long-term annealing. The annealing time may not have been sufficient to achieve steady-state by diffusion for samples with a high content of antimony. Since it was not possible to clearly determine which of these four phases is metastable, the results obtained in Tables II, III, and IV were retained.

Information about temperatures of phase transition in the Sb-Sn-Zn system was obtained only by using a Netzsch STA 409 DTA calorimeter. It is not possible to use a differential scanning calorimeter (DSC) for several reasons. Zinc evaporates from the Sb-Sn-Zn alloy samples during measurement and thus the overall composition of the samples is changing. Zinc also

Table III. The Overall Composition and Composition of Coexisting Phases at 523 K (250 °C)

	Overall Composition (at. pct)				Phases Composition (at. pct)		
Sample	Sb	Sn	Zn	Coexisting Phases	Sb	Sn	Zn
B1	14.53	13.98	71.50	liquid	1.01	86.15	12.92
				SbZn_Beta	44.76	2.82	53.24
				HCP_Zn	0.16	0.13	99.71
B2	59.55	17.57	22.88	Sb_2SnZn	50.25	25.75	24.01
				Rhombo_A7	90.43	9.30	0.27
				SbZn_Beta	52.5	0.27	47.23
B3	27.13	51.62	21.25	SbZn_Beta	51.63	0.53	47.84
				Sb_2SnZn	48.16	28.61	23.23
				liquid	6.01	91.68	2.31
B4	51.32	14.95	33.73	Sb_2SnZn	50.07	25.99	23.94
				SbSn	52.83	45.61	1.56
				SbZn_Beta	51.46	0.35	48.194
B5	18.81	1.18	4.64	liquid	0.91	87.47	11.62
				SbZn_Beta	43.98	1.36	54.66
				HCP_Zn	0.09	0.11	99.8
B6	66.03	27.04	6.93	Sb_2SnZn	51.64	25.52	22.84
				SbSn	58.77	40.64	0.59
				liquid	89.93	9.53	0.53
B7	38.99	21.68	39.33	SbZn_Beta	51.26	0.47	48.28
				liquid	1.13	85.43	13.45
				Sn4Zn6	1.37	36.77	61.85
B8	56.51	27.09	16.40	SbZn_Beta	52.66	0.29	47.05
				Sb_2SnZn	50.43	27.10	22.47
				SbSn	50.31	49.23	0.46
				Rhombo_A7	86.73	12.51	0.76
B9	50.46	22.88	26.66	SbZn_Beta	52.55	0.62	46.84
				Sb_2SnZn	50.35	25.83	23.83
				SbSn	49.66	49.93	0.41
B10	45.09	28.45	26.46	SbZn_Beta	52.60	0.29	47.11
				Sb_2SnZn	48.70	28.98	22.32
				liquid	7.07	89.872	3.058
B11	50.12	40.58	9.30	SbZn_Beta	52.70	0.44	46.86
				Sb_2SnZn	51.47	25.24	23.28
				SbSn	49.77	49.64	0.59
B12	20.24	71.33	8.43	Sb_2SnZn	49.69	27.26	23.05
				liquid	8.61	88.66	2.73
B13	41.68	50.20	8.11	Sb_2SnZn	50.65	26.09	23.25
				liquid	7.67	90.38	1.95
				SbSn	43.36	55.98	0.67

damages the metal parts of the detector in the DSC calorimeter. Moreover, Sb-Sn-Zn alloys react with oxygen in inert gas at elevated temperatures. The disadvantages of the DTA method are described in literature.[20] One of them is that the solid-phase transformation temperatures can be less reliable.

In the case of Sb-Sn-Zn alloy, the most appropriate technique is using the DTA with the samples sealed in evacuated quartz ampoules. The DTA signal (with repeated heating of individual sample) was well reproducible (see Figure 7) but too complex in most of the measurements. This is due to the fact that there are several phase transformations during heating and cooling. These phase transitions also have different kinetics. Samples were measured with the heating rate of 5 K/min. It was observed that some of the phase transitions take place easily (*i.e.*, the transformation signal during heating can be assigned to the corresponding signal in the cooling effect without undercooling), others show the effect of supercooling. Temperatures of significant changes in the DTA signal during heating (temperature markers) are listed in Table I.

The method of preparation of alloys in DTA quartz ampoules for measuring has been established. After the homogenization it is possible to carry out DTA measurement as well as subsequent long-term annealing in order to achieve phase equilibrium. Time saving was the greatest advantage.

The CALPHAD method was used to predict the isothermal section of the ternary phase diagram of the Sb-Sn-Zn system. Phase diagram was calculated using Pandat software. The binary thermodynamic parameters were used for this ternary prediction only (see line of phase boundaries in Figures 1, 2, and 3). The ternary phase Sb_2SnZn was omitted.

Table IV. The Overall Composition and Composition of Coexisting Phases at 623 K (350 °C)

	Overall Composition (at. pct)				Phases Composition (at. pct)		
Sample/Equilibrating Time	Sb	Sn	Zn	Coexisting Phases	Sb	Sn	Zn
C1	50.10	31.45	18.45	SbSn	50.10	49.75	0.42
1080 h				SbZn_Beta	52.55	0.34	47.11
				Sb_2SnZn	51.28	25.35	23.37
C2	52.15	38.71	9.14	SbSn	53.62	46.16	0.30
1080 h				SbZn_Beta	52.87	0.38	46.90
				Sb_2SnZn	51.54	25.97	22.48
C3	51.95	26.10	21.95	SbSn	52.89	46.99	0.34
1080 h				SbZn_Beta	52.88	0.42	46.71
				Sb_2SnZn	50.99	25.77	23.24
C4	68.17	20.48	11.35	SbSn	62.38	37.35	0.46
1080 h				Rhombo_A7	88.92	11.19	0.23
				Sb_2SnZn	51.47	25.53	22.99
				SbZn_Beta	52.84	0.52	46.68
C5	52.38	24.13	23.49	SbSn	55.71	44.12	0.17
9 h				SbZn_Beta	52.74	0.19	47.06
				Sb_2SnZn	51.43	24.97	23.56
C6	36.75	38.59	24.66	SbZn_Beta	52.25	0.35	47.40
500 h				Sb_2SnZn	48.80	28.27	22.93
				liquid	8.40	90.58	1.02
C7	46.55	9.95	43.50	SbZn_Beta	52.69	0.50	46.81
500h				liquid	0.74	85.68	13.58
C8	69.20	20.31	10.96	SbZn_Beta	52.74	0.34	46.92
500h				SbSn	59.85	39.90	0.25
				Sb_2SnZn	50.77	25.57	23.67
				rhombo_A7	91.21	7.98	0.81
C9	10.31	79.93	9.76	Sb_2SnZn	45.96	30.84	23.20
500 h				liquid	7.17	86.72	6.11
C10	43.95	44.00	12.05	Sb_2SnZn	50.88	25.69	23.42
500 h				liquid	7.17	86.72	6.11
				SbSn	48.36	51.15	0.48
C11	41.69	41.88	16.43	liquid	18.44	76.92	4.65
500 h				Sn_2SnZn	51.18	25.52	23.30
				SbSn	46.53	53.01	0.46

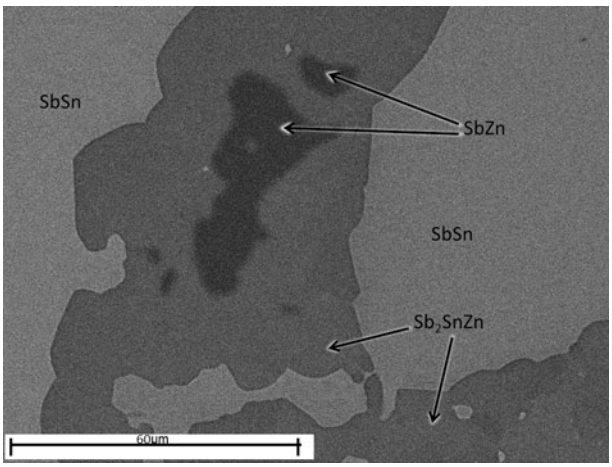

Fig. 4—Microstructure of sample C2 (see Table IV for composition). The equilibrated coexisting phases at 623 K (350 °C) can be easily distinguished by different shades of gray (SEM).

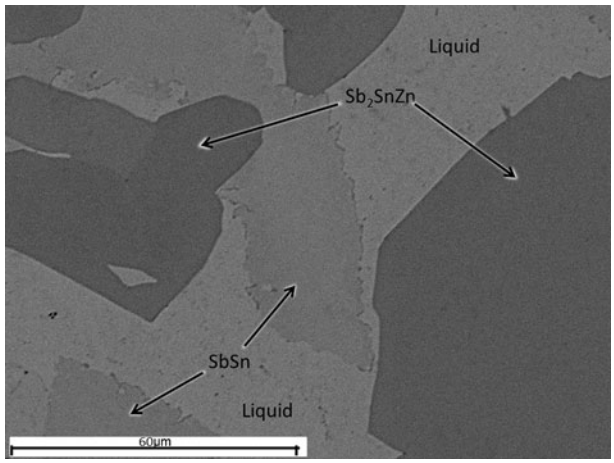

Fig. 5—Microstructure of sample C10 (see Table IV for composition, SEM). The ternary phase Sb_2SnZn and SbSn were at 623 K (350 °C) in equilibrium with the liquid phase before quenching in water.

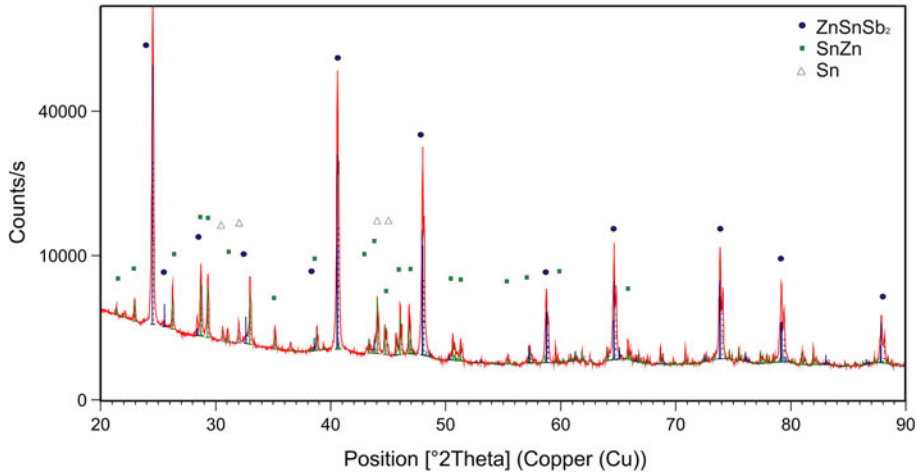

Fig. 6—X-ray diffraction spectrum for sample B10 after quenching to room temperature (see Table III for composition). Phases: SbZn_Beta (43653 HCSD, 24 wt pct), Sb_2SnZn (42669HCSD, 75 wt pct), and βSn (40037 HCSD, transformed liquid phase, 2 wt pct).

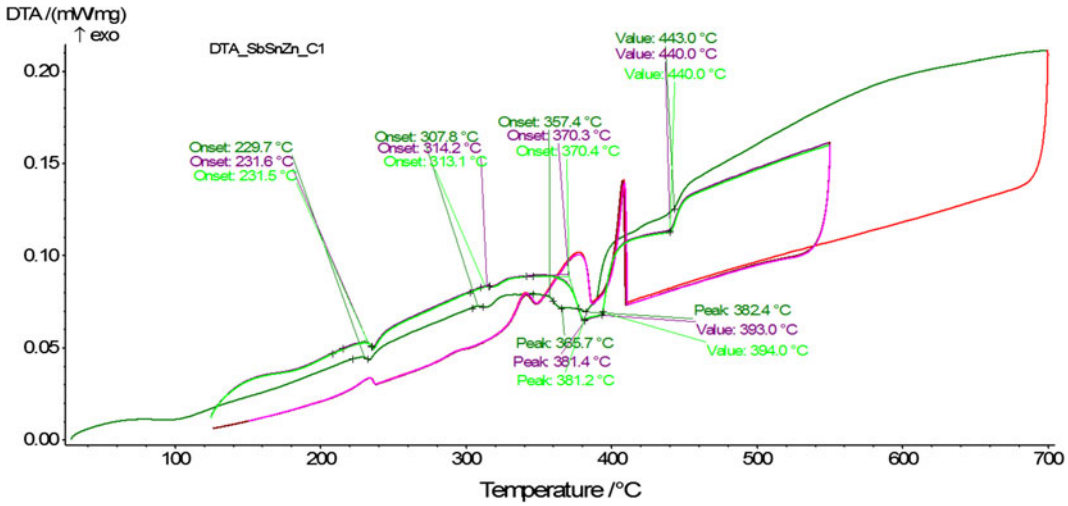

Fig. 7—DTA signal (two identical heating and cooling cycles) of the sample C1 with phase transitions markers (Tables I and IV for composition).

IV. CONCLUSIONS

The coexistence of the phases Sb-Sn-Zn alloy system was observed at three different temperatures of 473 K, 523 K, and 623 K (200 °C, 250 °C, and 350 °C). The composition of the coexisting phases was measured for the monitored samples. The experiment was extended also to dynamic measurement using DTA. The data about not only liquidus temperature but also other phase transformations were obtained by DTA measurement. Existence of the ternary phase Sb_2SnZn in the monitored system was confirmed. Another ternary phase was not found. The presented results are applicable to the construction of equilibrium phase diagram of Sn-Sb-Zn system and an assessment using CALPHAD approach.

ACKNOWLEDGMENTS

Financial support of the Ministry of Education of the Czech Republic (Project COST 0903 Action MP0903 (LD 11046), RVO: 68081723, and CEITEC-MU CZ.1.05/1.1.00/02.0068 are gratefully acknowledged.

REFERENCES

1. Y. Lin, L.Q. Yin, and X.C. Wei: *2011 12th Int. Conf. Electron. Packag. Technol. High Density Packag. (Icept-Hdp)*, 2011, pp. 338–41.
2. G. Zeng, S. McDonald, and K. Nogita: *Microelectron. Reliab.*, 2012, vol. 52, pp. 1306–22.

3. H. Ma and J.C. Suhling: *J. Mater. Sci.*, 2009, vol. 44, pp. 1141 58.
4. V. Kumar, Z.Z. Fang, J. Liang, and N. Dariavach: *Metall. Mater. Trans. A*, 2006, vol. 37A, pp. 2505–14.
5. T.C. Chang, M.C. Wang, and M.H. Hon: *Metall. Mater. Trans. A*, 2005, vol. 36A, pp. 3019–29.
6. D.R. Frear and P.T. Vianco: *Metall. Mater. Trans. A*, 1994, vol. 25A, pp. 1509–23.
7. A. Dinsdale, A. Watson, A. Kroupa, J. Vrestal, A. Zemanova, and J. Vizdal: in *Atlas of Phase Diagrams for Lead-Free Soldering*, COST Office, Brussels, 2008.
8. J.B. Li, M.C. Record, and J.C. Tedenac: *J. Alloys. Compd.*, 2007, vol. 438, pp. 171–77.
9. S.W. Chen, C.C. Chen, W. Gierlotka, A.R. Zi, P.Y. Chen, and H.J. Wu: *J. Electron. Mater.*, 2008, vol. 37, pp. 992–1002.
10. V.A. Khudolii, M.I. Golovei, and A.V. Novoselova: *Dokl. Akad. Nauk. Sssr.*, 1976, vol. 228, pp. 1126–27.
11. A. Tenga, F.J. Garcia-Garcia, A.S. Mikhaylushkin, B. Espinosa-Arronte, M. Andersson, and U. Haussermann: *Chem. Mater.*, 2005, vol. 17, pp. 6080–85.
12. T. Gancarz and W. Gasior: *J. Phase Equilib. Diffus.*, 2011, vol. 32, pp. 398–406.
13. N.A. Goryunova, B.V. Baranov, V.S. Grigoryeva, L.V. Kradinova, F.A. Maksimova, and V.D. Prochukhan: *Izv. Akad. Nauk. SSSR Neorg. Mater.*, 1968, vol. 4, p. 1060.
14. W. Scott: *J. Appl. Phys.*, 1973, vol. 44, pp. 5165–66.
15. L. Kaufman and H. Bernstein: *Computer Calculation of Phase Diagrams with Special Reference to Refractory Metals*, Academic Press, New York, 1970.
16. N. Saunders and A.P. Miodownik: *CALPHAD (Calculation of Phase Diagrams): A Comprehensive Guide*, Pergamon, Oxford, 1998.
17. S. Pingfang and B. Sundman: *TCC*™ Thermo-Calc Software User's Guide, Version N, Foundation of Computational Thermodynamics, Stockholm, 2002.
18. S.L. Chen, F. Zhang, S. Daniel, F.Y. Xie, X.Y. Yan, Y.A. Chang, R. Schmid-Fetzer, and WA Oates: *JOM.*, 2003, vol. 55, pp. 48–51.
19. O. Zobač and J. Sopoušek: Bachelor's Theses, Masaryk university, Faculty of science, 2010.
20. W.J. Boettinger, K.U.R., M.K. Won, and P. John: ''NIST Recommended Practice Guide: DTA and Heat-Flux DSC Measurements of Alloy Melting and Freezing'', National Institute of Standards and Technology, 2006.
21. A. Ulichová: Diploma Thesis (Mgr.), Masaryk university, Faculty of science, 2009.